Hindawi Publishing Corporation
EURASIP Journal on Embedded Systems
Volume 2007, Article ID 46972, 8 pages
doi:10.1155/2007/46972

*Research Article*

# Lane Tracking with Omnidirectional Cameras: Algorithms and Evaluation

**Shinko Yuanhsien Cheng and Mohan Manubhai Trivedi**

*Laboratory for Intelligent and Safe Automobiles (LISA), University of California, San Diego, La Jolla, CA 92093-0434, USA*

Received 13 November 2006; Accepted 29 May 2007

Recommended by Paolo Lombardi

With a panoramic view of the scene, a single omnidirectional camera can monitor the 360-degree surround of the vehicle or monitor the interior and exterior of the vehicle at the same time. We investigate problems associated with integrating driver assistance functionalities that have been designed for rectilinear cameras with a single omnidirectional camera instead. Specifically, omnidirectional cameras have been shown effective in determining head gaze orientation from within a vehicle. We examine the issues involved in integrating lane tracking functions using the same omnidirectional camera, which provide a view of both the driver and the road ahead of the vehicle. We present analysis on the impact of the omnidirectional camera's reduced image resolution on lane tracking accuracy, as a consequence of gaining the expansive view. And to do so, we present Omni-VioLET, a modified implementation of the vision-based lane estimation and tracking system (VioLET), and conduct a systematic performance evaluation of both lane-trackers operating on monocular rectilinear images and omnidirectional images. We are able to show a performance comparison of the lane tracking from Omni-VioLET and Recti-VioLET with ground truth using images captured along the same freeway road in a specified course. The results are surprising: with 1/10th the number of pixels representing the same space and about 1/3rd the horizontal image resolution as a rectilinear image of the same road, the omnidirectional camera implementation results in only three times the amount the mean absolute error in tracking the left lane boundary position.



## 1. INTRODUCTION: OMNIDIRECTIONAL CAMERA FOR LOOKING IN AND LOOKING OUT

Omnidirectional camera's main feature is its ability to capture an image of the scene 360 degrees around the camera. It has the potential to monitor many things in the scene at one time, illustrated in Figure 1. In an intelligent driver assistance system, this means a single sensor has the potential to monitor the front, rear, and side views of vehicle and even inside the vehicle simultaneously. This eliminates the need for multiple cameras and possibly complex calibration maintenance algorithms between multiple cameras. Due to the fact that reducing redundancy is one of the main goals in embedded systems, combining multiple functionalities into a single, simpler sensor reduces the cost associated with maintaining individual sensors for each sensing function.

There is also evidence that driver behavior should be an integral part of any effective driver assistance system [1], driving the need for a suite of sensors that extracts cues from both outside and inside the vehicle. With these motivations, we investigate problems associated with integrating driver assistance functionalities that have been designed for multiple rectilinear cameras on a single omnidirectional camera instead. For this paper, we examine issues involved in and suggest solutions to integrate lane tracking functions using the omnidirectional camera in this multifunction context.

Huang et al. [2] demonstrated that an omnidirectional camera can be used to estimate driver head pose to generate the driver's view of the road. Knowledge of the driver's gaze direction has of course many uses beyond driver-view synthesis. The driver head motion is the critical component that added one second of warning time to a lane departure warning system in [3]. This human-centered driver support system uses vehicle lane position from cameras looking out of the vehicle, vehicle speed, steering, yaw rate from the vehicle itself, as well as head motion from a camera looking in the vehicle to make predictions of when drivers make lane-change maneuvers. Estimates of driver head movement also improved intersection turn maneuver predictions [4]. There, each of these predictions can potentially describe the driver's

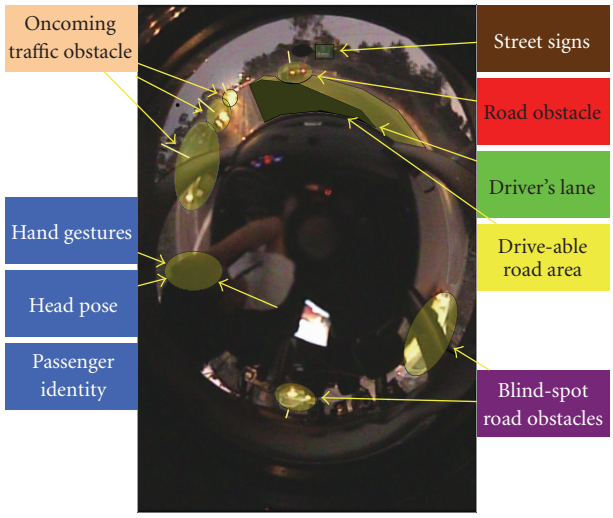


Figure 1: This figure shows an illustrative image captured by omnidirectional cameras and the panoramic field of view with a potential for holistic visual context analysis.

awareness of the driving situation. For example, given an obstacle in the vehicle's path and continued driver preparatory movements to perform the maneuver, the assistance system can then conclude that the driver is unaware of the danger and take appropriate action. Observing the driver also has applications in driver identity verification, vigilance monitoring, along with intention and awareness monitoring. It is clear that driver bodily movements are very significant cues in determining several driver behaviors. It is also clear that visual methods using omnidirectional cameras of extracting some of this driver information have been shown to be an effective approach.

In addition to head pose, lane tracking is also an important component in many intelligent driver assistance systems. Lane tracking has utility in lane departure warning, overspeed warnings for sharp curves, ahead vehicle proximity estimation for adaptive cruise control, collision avoidance, obstacle detection, and many others [5]. Just as observing drivers will enhance driving safety, lane tracking is an integral part in the same task.

This naturally leads to the following question: can efficiency be improved by utilizing a single omnidirectional camera rather than two rectilinear cameras to perform these same functions of observing the driver and the road? Since the only difference between rectlinear and omnidirectional images is the projection function, that is, the manner in which 3D points in space are projected onto the 2D image plane, the answer should be yes. The question is to what extent. We attempt to answer these questions by comparing the results between VioLET, a vision-based lane estimation and tracking system [6] operating on rectlinear images, and Omni-VioLET, a modified version operating on omnidirectional images. We compare the tracking results from both systems with ground truth. Our contributions can be listed in the following:

(1) we introduce a lane tracking system using an omnidirectional camera that utilizes a well-tested, robust lane tracking algorithm called Omni-VioLET. The omnidirectional camera also captures a view of the driver at the same time for driver monitoring applications;
(2) we discuss and undertake a systematic performance comparison of the lane tracking systems using a rectilinear camera and omnidirectional camera of the same road course with ground truth.

## 2. RELATED RESEARCH IN VISION-BASED LANE TRACKING

Most previously proposed vision-based lane tracking systems follow a processing structure consisting of these three steps: (1) extract road features from sensors, (2) suppress outliers from the extracted road features, and (3) estimate and track lane model parameters.

There are several notable lane tracking approaches using rectilinear cameras. The one by Bertozzi and Broggi [7] proposes to use stereo rectilinear camera for lane detection combined with obstacle detection. They employ a flat-plane transformation of the image onto a birds-eye view of the road, followed by a series of morphological filters to locate the lane markings. A recent contribution by Nedevschi et al. [8] augments the usual flat-plane assumption of the road to a 3D model based on clothoids and vehicle roll angles. That system relies on depth maps calculated from a stereo camera and edges in images to infer the orientation of the 3D road model. A detailed survey of lane position and tracking techniques using monocular rectilinear cameras is presented in [6].

Ishikawa et al. [9] proposes an approach using an omnidirectional camera to track lane position in an autonomous vehicle application. The approach first transforms the omni-image to flat-plane, followed by Hough transform to search for the left and right lane marking with a lane separation prior. With an autonomous vehicle application in mind, the scene captured by this omnidirectional camera saw lane markers ahead and behind the vehicle, both aiding in determining the vehicle's position in the lane and lane width. Furthermore, lines perpendicular to the vehicle could also be detected with this system since the sides are also monitored as well. This work demonstrates that effective lane tracking can be achieved to some extent with omnidirectional images.

Because the Ishikawa approach was designed in the context of autonomous vehicles, the operating environment, although the setting was outdoors, was idealized with solid white lines for lane markings with constant lane widths. The central component of the VioLET system is the use of steerable filters, which has been shown to be highly effective in extracting circular reflectors as well as line segments, prevalent lane markings in actual California freeways. Furthermore, the algorithm lacked a mechanism to incorporate temporal history of last observed lane locations with the current estimate. We will use the Kalman filtering framework to update interesting statistics of lane position, lane width, and so forth using lane position measurements from the current as well as previous moments in time. Lastly, we are interested in

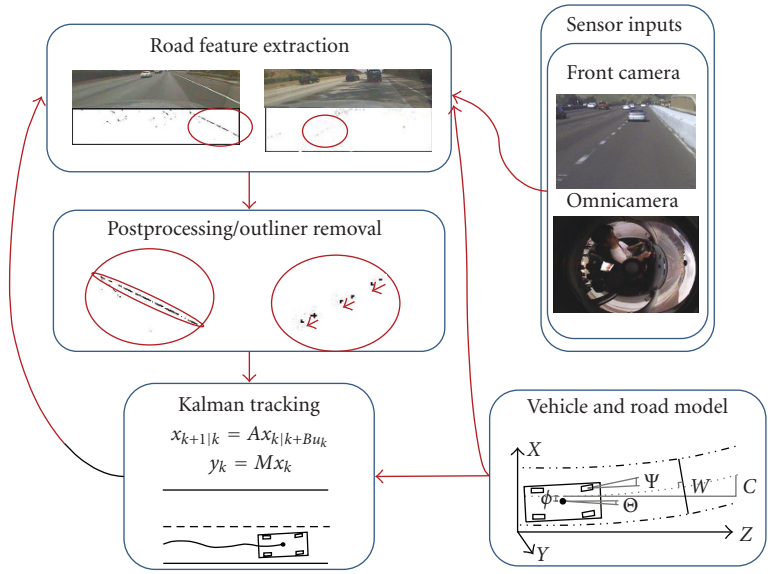


FIGURE 2: This illustrates the system flow diagram for VioLET, a driver-assistance focused lane position estimation and tracking system.

examining the extent to which lane tracking can be accurate by using only the view of the road ahead of the vehicle, deferring the other areas of the omnidirectional image for other applications that monitor the vehicle interior.

## 3. OMNI-VIOLET LANE TRACKER

In this section, we describe the modifications to the VioLET system for operation on omnidirectional images. An omnidirectional camera is positioned just below and behind the rear view mirror. From this vantage point, both the road ahead of the vehicle as well as the front passengers can be clearly seen. With this image, left lane marker position, right lane marker position, vehicle position within the lane, and lane width are estimated from the image of the road ahead. Figure 2 shows a block diagram of the Omni-VioLET system for use in this camera comparison.

The VioLET system operates on a flat-plane transformed image, also referred to as a birds-eye view of the road. This is generated from the original image captured from the camera, with knowledge of the camera's intrinsic and extrinsic parameters and orientation of the camera with respect to the ground. The intrinsic and extrinsic parameters of the camera describe the many-to-one relationship between the 3D points in the scene in real-world length units and its projected 2D location on the image in image pixel coordinates. The planar road assumption allows us to construct a one-to-one relationship between 3D points on the road surface and its projected 2D location on the image in image pixel coordinates. This is one of the critical assumptions that allow lane tracking algorithms to provide usable estimates of lane location and vehicle position, and is also the assumption utilized in the VioLET system.

The model and calibration of rectilinear cameras are very well studied, and many of the results translate to omnidirectional cameras. We can draw direct analogs between the omnidirectional camera model and the rectilinear camera model, namely its intrinsic and extrinsic parameters. Tools for estimating the model parameters have been also recently made available [10]. Table 1 summarizes the transformations from a 3D point in the scene $\mathbf{P} = (x, y, z)$ to the projected image point on the image $\mathbf{u} = (u, v)$.

Utilizing the camera parameters for both rectilinear and omnidirectional cameras, a flat-plane image can be generated given knowledge of the world coordinate origin and the region on the road surface we wish to project the image onto. The world origin is set at the center of the vehicle on the road surface with the $y$-axis pointing forward and $z$-axis pointing upward. Examples of the flat-plane transformation are shown in Figure 3. Pixel locations of points in the flat-plane image and the actual locations on the road are related by a scale factor and offset.

The next step is extracting road features by applying steerable filters based on the second derivatives of a two-dimensional Gaussian density function. Two types of road features are extracted: circular reflectors ("Bots dot") and lines. The circular reflectors are not directional so the filter responses are equally high in both the horizontal and vertical directions. The lines are highly directional and yield high responses for filters oriented along its length. The filtered images such as the one shown in Figure 3 are then thresholded and undergo connected component analysis to isolate the most likely candidate road features.

The locations of the road features are averaged to find the new measurement of the lane boundary location. The average is weighted on its proximity to the last estimated location of the lane boundary. The measurement for the other lane boundary is made the same way. The last estimated lane boundary location is estimated using a Kalman filter using lane boundary locations as observations, and vehicle position

Table 1: Projective transformation for rectilinear and omnidirectional cameras.

| | Rectilinear camera model | Omnidirectional catadioptric camera model |
|---|---|---|
| World to camera coordinates | $\mathbf{P}_c = \begin{pmatrix} X_c \\ Y_c \\ Z_c \end{pmatrix} = \mathbf{RP} + \mathbf{t}$ | $\mathbf{P}_c = \begin{pmatrix} X_c \\ Y_c \\ Z_c \end{pmatrix} = \mathbf{RP} + \mathbf{t}$ |
| Camera to homogeneous camera plane (normalized camera) coordinates | $\mathbf{p}_n = \begin{pmatrix} x_n \\ y_n \end{pmatrix} = \begin{pmatrix} X_c/Z_c \\ Y_c/Z_c \end{pmatrix}$ | — |
| Undistorted to distorted camera plane coordinates | $\mathbf{p}_d = \begin{pmatrix} x_d \\ y_d \end{pmatrix} = \lambda \mathbf{p}_n + dx,$ $\lambda = 1 + \kappa_1 r^2 + \kappa_2 r^4 + \kappa_3 r^6,$ $dx = \begin{pmatrix} 2\rho_1 xy + \rho_2(r^2 + 2x^2) \\ \rho_1(r^2 + 2y^2) + 2\rho_2 xy \end{pmatrix},$ $r^2 = x_n^2 + y_n^2$ | $\begin{pmatrix} x_d \\ y_d \\ f(x_d, y_d) \end{pmatrix} = \begin{pmatrix} X_c \\ Y_c \\ Z_c \end{pmatrix},$ $f(x_d, y_d) = a_0 + a_1\rho + a_2\rho^2 + a_3\rho^3 + a_4\rho^4,$ $\rho^2 = x_d^2 + y_d^2$ |
| Distorted camera plane to image coordinates | $\begin{pmatrix} u \\ v \\ 1 \end{pmatrix} = \begin{pmatrix} f_x & \alpha f_x & c_x \\ 0 & f_y & c_y \\ 0 & 0 & 1 \end{pmatrix} \begin{pmatrix} x_d \\ y_d \\ 1 \end{pmatrix}$ | $\begin{pmatrix} u \\ v \\ 1 \end{pmatrix} = \begin{pmatrix} f_x & \alpha f_x & c_x \\ 0 & f_y & c_y \\ 0 & 0 & 1 \end{pmatrix} \begin{pmatrix} x_d \\ y_d \\ 1 \end{pmatrix}$ |

in the lane, left lane boundary location, right lane boundary location, and lane width as hidden states. For more details on these steps of extracting road features and tracking these features using the Kalman filter we refer the reader to the original paper [6]. The original implementation also takes advantage of vehicle speed, yaw-rate, and road texture to estimate road curvature and refine the estimates of the lane model. We chose to omit those measurements in our implementation, and to focus on estimating lane boundary position and vehicle position in the lane, for which ground truth can be collected, to illustrate the point that omnidirectional cameras have the potential to be used for lane tracking.

Altogether, the VioLET system assumes a planar road surface model, knowledge of camera parameters, road feature extraction using steerable filters, and the lane model parameters are tracked with a Kalman filter using road feature location measurements as observations. The outputs are lane boundary positions, lane width, and vehicle position in the lane.

## 4. EXPERIMENTAL PERFORMANCE EVALUATION AND COMPARISON

Omni-VioLET lane tracking system is evaluated with video data collected from three cameras in a specially equipped Laboratory for Intelligent and Safe Automobiles-Passat (LISA-P) test vehicle. A rectilinear camera placed on the roof of the car and the omnidirectional camera hung over the rear-view mirror capture the road ahead of the vehicle. A third camera is used to collect ground truth. All cameras are Hitachi DP-20A color NTSC cameras, and $720 \times 480$ RGB images are captured via a Firewire DV capture box to a PC at 29.97 Hz. The vehicle was driven along actual freeways and video was collected synchronously along with various vehicle parameters. Details of the test-bed can be found in [4].

For evaluation, we collected ground truth lane position data using the third calibrated camera. A flat-plane image from this camera is also generated such that the horizontal position of the transformed image represents the distance from the vehicle. A grid of points corresponding to known physical locations of the ground is used to adjust the orientation and position of the side camera. Figure 4 shows the result of manually correcting the pose of the camera, and thus the grid of points in the image from the side camera. With this grid of points and its associated location in the image, a flat-plane image is generated as shown in the same figure. From the flat-plane image, lane positions are manually annotated to generate ground truth. This ground truth is compared against lane tracking results of both the rectilinear and omnidirectional VioLET systems.

The lane tracking performance is analyzed on data collected from a test vehicle driven at dusk on a multilane freeway at freeway speeds for several minutes. It was shown that dusk was one of the many times during a 24-hour period when VioLET performed most optimally, because of the light traffic conditions [6]. This allows a comparison of the omni-image based lane tracking with the most optimal rectilinear image-based lane tracking results. The image resolution of the flat-plane transformed image derived from the omnicamera was set at $100 \times 100$, while the one derived from the rectilinear-image was set at $694 \times 2000$. For the omni-case, that resolution was chosen because the lateral resolution of the road is approximately 100 pixels wide. For the rectilinear case, the lateral resolution is slightly shorter than the

Table 2: Lane tracking accuracy. All units are in cm.

| | Lane following (RMSE/MAE) | Lane changing (RMSE/MAE) | Overall (RMSE/MAE) |
|---|---|---|---|
| Omni-VioLET | 3.5/4.7 | 3.9/4.2 | 4.7/4.4 |
| Recti-VioLET full-res. (720 × 480) | 1.3/1.5 | 6.1/5.5 | 5.9/4.5 |
| Recti-VioLET half-res. (360 × 240) | 1.7/2.2 | 5.3/5.2 | 5.1/4.2 |
| Recti-VioLET qtr-res. (180 × 120) | 1.5/2.1 | 5.7/6.7 | 5.6/4.9 |
| Recti-VioLET eighth-res. (90 × 60) | 1.6/2.2 | lost-track** | lost-track** |

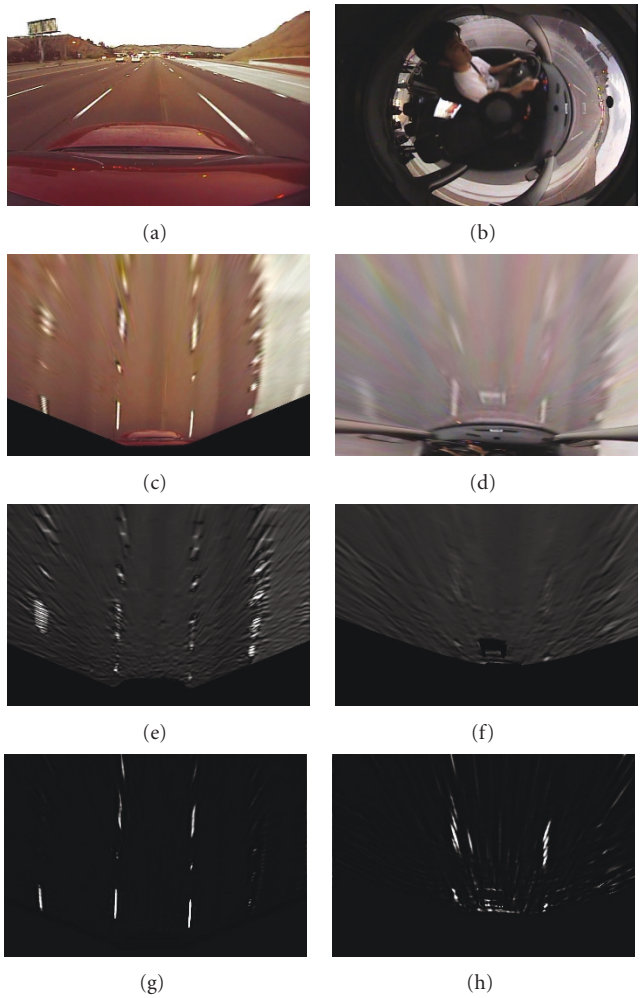

Figure 3: This illustration shows the original images, the flat-plane transformed images, and two filter response images from the flat-plane transformed images for circular reflectors and lane line markers.

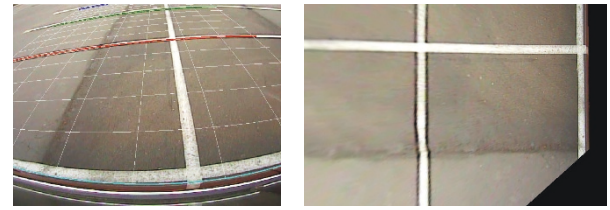

Figure 4: This illustrates the alignment of the ground-grid to the perceived ground in the ground-truth camera, and the resulting flat-plane transformed image. Radial distortion is taken into account as can be seen by the bowed lines.

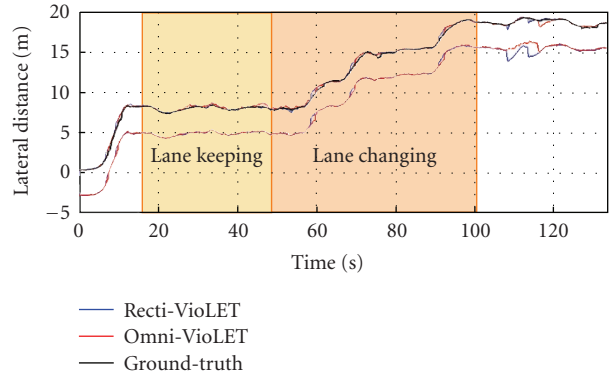


Figure 5: This figure depicts the progression of the lane-boundary estimates over time as found by the (full-resolution) rectilinear camera-based lane tracking, omnidirectional camera-based lane tracking and ground-truth. The shaded regions demarcate the lane-keeping and lane-changing segments of the road.

width of the 720 pixel-wide horizontal resolution of the image. The vertical resolution was chosen by making road features square, up to 100 feet forward of the camera.

In aligning lane tracking results from the two systems with ground-truth, the ground-truth is kept unchanged for reference. The lane tracking estimates were manually scaled and offset to compensate for errors in camera calibration, camera placement, and error in lane-width estimation. This alignment consists of three operations on the lateral lane boundary and lane position estimates: (1) global offset, (2) global scale, and (3) unwrapping amount. The global offset puts all 3 cameras on the same lateral position of the car. The global scale changes the scale of the estimates which result from errors in camera calibration. Unwrapping amount is specified to compensate for errors in lane-width estimates, which impact left-lane position estimates when the left-lane location is more than half a lane-width away. These alignment parameters are set once for the entire experiment. The resulting performance characteristics are shown as error in centimeters.

It is important to note that these error measurements are subject to errors in the ground-truth-camera calibration accuracy. Indeed, an estimate that closely aligns with ground-truth can be claimed to be only that. In this particular case, a scaling error in ground-truth calibration could result in a

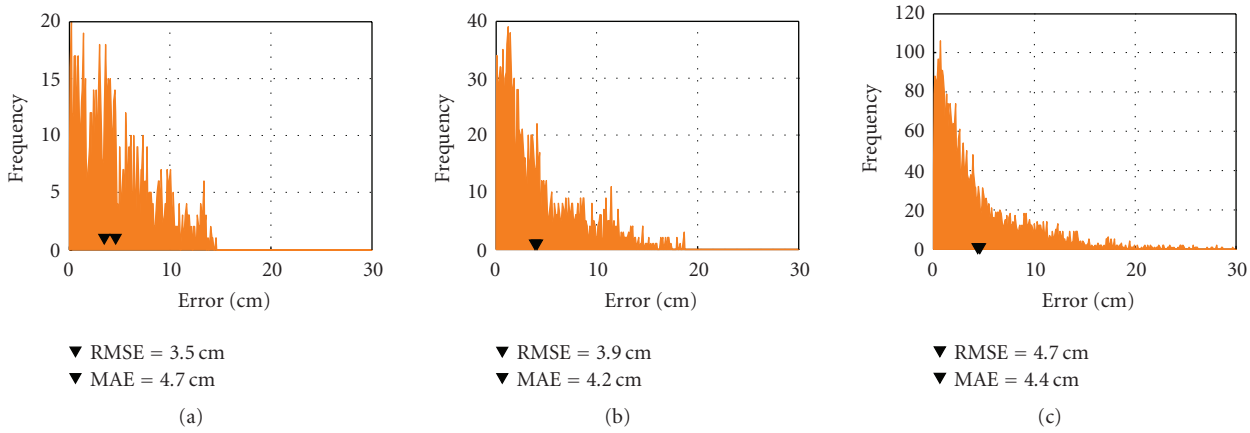


Figure 6: The illustration shows the distribution of error of the omnidirectional camera-based lane tracking from ground-truth during (a) the lane keeping segment, (b) the lane changing segment, and (c) the overall ground-truthed test sequence.

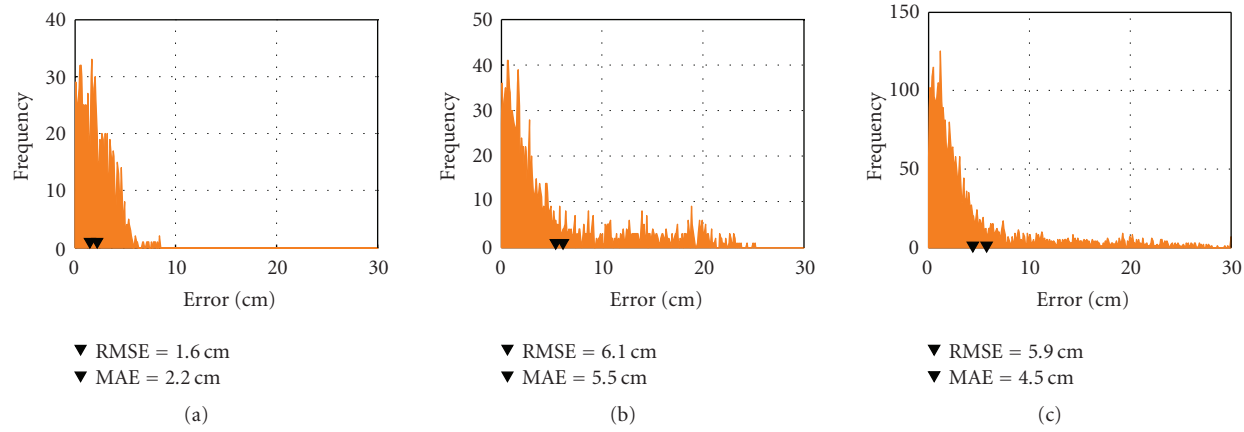


Figure 7: The illustration shows the distribution of error of the rectilinear camera-based lane tracking from ground-truth during (a) the lane keeping segment, (b) the lane changing segment, and (c) the overall ground-truthed test sequence.

scaling error in the lane tracking measurements. This would be the case for any sort of vision-based measurement system using another vision-based system to generate ground-truth. For the ground-truth camera used in our experiments, we approximate a deviation of ±5 cm of the model to the actual location in the world by translating the model ground plane and visually inspecting the alignment with two 2.25 m parking slots; see Figure 4. With that said, we can however make conclusions about the relative accuracies between two lane-tracking systems, which we present next.

Several frames from the lane tracking experiment are shown in Figures 8 and 9. The top set of images show the even and odd fields of the digitized NTSC image, while the bottom set of images show the lane tracking result showing the lane feature detection in boxes and left and right lane boundary estimates in vertical lines. The original image was separated because each image was captured at 1/60 second from each other, which translates to images captured at positions 50 cm apart with the vehicle traveling 30 m/s (65 mph). Figure 5 shows results of estimates over time of left and right lane boundaries from both systems against left-lane boundary ground-truth during two segments of one test run. Two segments of lane-following and lane-changing manuevers are analyzed separately. The error distributions are shown in Figures 6 and 7. In these two segments, we can see the strength of the rectilinear camera at approximately 1.5 cm mean absolute error (MAE) from ground-truth as compared to omnidirectional camera-based lane tracking performance of 4.2 cm MAE. During a lane change maneuver, the distinction is reversed. The two systems performed with 5.5 cm and 4.2 cm MAE, respectively; root mean square (RMS) error shows the same relationship. Over the entire sequence, the errors were 4.5 cm and 4.4 cm MAE and 5.9 cm and 4.7 cm RMS error for Recti-VioLET and Omni-VioLET, respectively. Errors are summarized in Table 2.

During the lane-change segment, a significant source of error in both systems is the lack of a vehicle heading estimate. Rather, the lanes are assumed to be parallel with the vehicle as can be seen from the lane position estimate overlaid on the flat-plane images in Figures 8 and 9, which is of course

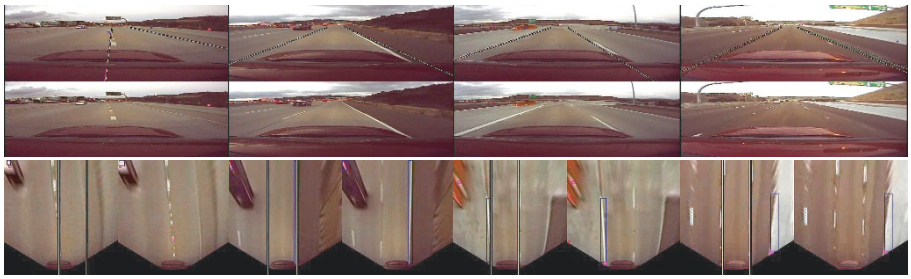

Figure 8: This illustrates the lane tracking results from rectilinear images. The top and middle images are the even and odd fields of the original NTSC image. The bottom two images are the flat-plane transformed images of the above two images. The two overlay lines depict the estimated left and right lane positions while the boxes represent detected road features.

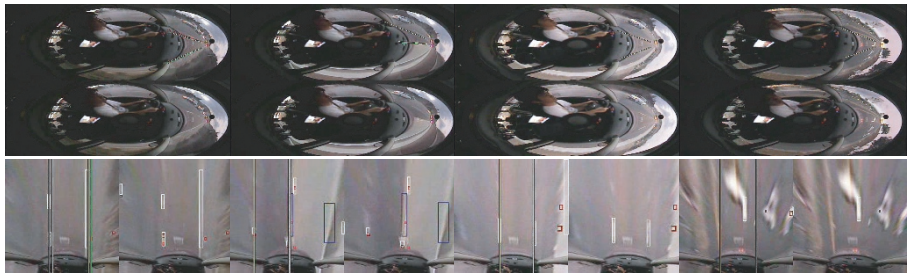

Figure 9: This illustrates the lane tracking results from omnidirectional images. The top and middle images are the even and odd fields of the original NTSC image. The bottom two images are the flat-plane transformed images of the above two images. The two overlay lines depict the estimated left and right lane positions while the boxes represent detected road features.

not always the case. For that reason, we gauge the relative accuracy between Recti-VioLET and Omni-VioLET along the lane following sequence. Despite the curves in the road, this segment could show that the diminished omni-image resolution resulted in a mere 3 times more MAE.

Additional runs of Recti-VioLET were conducted on half, quarter, and eighth resolution rectilinear images. The size of the flat-plane transformation is maintained at $694 \times 2000$. At a quarter of the original resolution ($180 \times 120$), the lateral road resolution in the rectilinear image is approximately equal to that of the omni-image. The resulting accuracies are summarized in Table 2. Remarkable is their similar performance even at the lowest resolution. To determine lane boundary locations, several flat-plane marking candidates are selected and its weighted average along the lateral position serves as the lane boundary observation to the Kalman tracker. This averaging could explain the resulting subpixel accurate estimates. Only at the very lowest resolution (eighth) input image was the algorithm unable to maintain tracking of lanes across several lane changes. However, eighth-resolution lane tracking in lane following situation yielded similar accuracies as lane tracking at the other resolutions.

Resolution appears to play only a partial role in influencing accuracy of lane tracking. The lane-markings detection performance appears to suffer increased number of misdetections at low resolution. This error appears in the accuracy measurements in the form of lost tracks through lane changes. Accuracy seems to not be affected by the reduced resolution. At resolutions of $180 \times 120$, misdetections occurred infrequently enough to maintain tracking throughout the test sequence. Lane-marking detection performance itself in terms of detection rate and false alarms at these various image resolutions and image types would give a better picture of the overall lane tracking performance; this is left for future work.

## 5. SUMMARY AND CONCLUDING REMARKS

We investigate problems associated with integrating driver assistance functionalities that have been designed for rectilinear cameras with a single omnidirectional camera instead. Specifically, omnidirectional cameras have been shown effective in determining head gaze orientation from within a car. We examined the issues involved in integrating lane-tracking functions using the same omnidirectional camera. Because the resolution is reduced and the image distorted to produce a 360-degree view of the scene through a catadioptric camera geometry as opposed to the traditional pin-hole camera geometry, the achievable accuracy of lane tracking is a question in need of an answer. To do so, we presented Omni-VioLET, a modified implementation of VioLET, and conducted a systematic performance evaluation of the vision-based lane estimation and tracking system operating on both monocular rectilinear images and omnidirectional images. We were able to show a performance comparison of the lane tracking from

Omni-VioLET and Recti-VioLET with ground-truth using images captured along the same freeway. The results were surprising: with 1/10th the number of pixels representing the same space and about 1/3rd the horizontal image resolution as a rectilinear image of the same road, the omnidirectional camera implementation results in only twice the amount of the mean absolute error in tracking the left-lane boundary position.

Experimental tests showed that the input image resolution is not the sole factor affecting accuracy, but it does have an impact on lane marking detection and maintaining track. The nearly constant error for full, half, quarter, and eighth resolution input images implied that accuracy is not affected by resolution; we attributed the ability of the algorithm to maintain this accuracy to the temporal averaging from Kalman filtering and the large flat-plane image used for all Recti-VioLET tests. The experiments affirm the result that lane tracking with omnidirectional images is feasible, and is worth consideration when a system utilizing a minimal number of sensors is desired.

## REFERENCES

[1] L. Petersson, L. Fletcher, A. Zelinsky, N. Barnes, and F. Arnell, "Towards safer roads by integration of road scene monitoring and vehicle control," *International Journal of Robotics Research*, vol. 25, no. 1, pp. 53–72, 2006.

[2] K. S. Huang, M. M. Trivedi, and T. Gandhi, "Driver's view and vehicle surround estimation using omnidirectional video stream," in *Proceedings of IEEE Intelligent Vehicles Symposium (IV '03)*, pp. 444–449, Columbus, Ohio, USA, June 2003.

[3] J. McCall, D. Wipf, M. M. Trivedi, and B. Rao, "Lane change intent analysis using robust operators and sparse Bayesian learning," to appear in *IEEE Transactions on Intelligent Transportation Systems*.

[4] S. Y. Cheng and M. M. Trivedi, "Turn-intent analysis using body pose for intelligent driver assistance," *IEEE Pervasive Computing*, vol. 5, no. 4, pp. 28–37, 2006.

[5] W. Enkelmann, "Video-based driver assistance—from basic functions to applications," *International Journal of Computer Vision*, vol. 45, no. 3, pp. 201–221, 2001.

[6] J. C. McCall and M. M. Trivedi, "Video-based lane estimation and tracking for driver assistance: survey, system, and evaluation," *IEEE Transactions on Intelligent Transportation Systems*, vol. 7, no. 1, pp. 20–37, 2006.

[7] M. Bertozzi and A. Broggi, "GOLD: a parallel real-time stereo vision system for generic obstacle and lane detection," *IEEE Transactions on Image Processing*, vol. 7, no. 1, pp. 62–81, 1998.

[8] S. Nedevschi, R. Schmidt, T. Graf, et al., "3D lane detection system based on stereovision," in *Proceedings of the 7th International IEEE Conference on Intelligent Transportation Systems (ITSC '04)*, pp. 161–166, Washington, DC, USA, October 2004.

[9] K. Ishikawa, K. Kobayashi, and K. Watanabe, "A lane detection method for intelligent ground vehicle competition," in *SICE Annual Conference*, vol. 1, pp. 1086–1089, Fukui, Japan, August 2003.

[10] D. Scaramuzza, A. Martinelli, and R. Siegwart, "A flexible technique for accurate omnidirectional camera calibration and structure from motion," in *Proceedings of the 4th IEEE International Conference on Computer Vision Systems (ICVS '06)*, p. 45, New York, NY, USA, January 2006.